

# INJECTED BEAM IMAGING AT SPEAR 3 WITH A DIGITAL OPTICAL MASK\*

H. Zhang<sup>#</sup>, R. Fiorito, and A. Shkvarunets, University of Maryland, College Park, MD, USA  
J. Corbett, K. Tian and A. Fisher, SLAC, Menlo Park, CA, USA

## Abstract

At SPEAR3, the 3GeV synchrotron light source operates in top-up injection mode with 273nC charge circulating in the storage ring (350mA). Each individual injection pulse contains only 40-80 pC, or a contrast ratio between stored to injected charge about 5000:1. In order to monitor injected beam dynamics during user operations, it is desirable to optically image the injected charge distribution on a turn-by-turn basis in the presence of the bright stored beam. The measurement is made by imaging the beam in visible synchrotron radiation onto a digital micro-mirror-array device (DMD) which is used to 'mask' light from the central stored beam while observing the weak injected beam signal on an image intensified, fast-gated CCD camera. Complex beam dynamics are observed after only a few tens of turns around the synchrotron. In this paper we report on the DMD optical configuration, masking considerations, measurement timing and initial tests imaging the injected beam in the presence of stored beam.

## INTRODUCTION

Previously, we have implemented a novel masking method to image beam halo with a high dynamic range at the University of Maryland Electron Ring (UMER) [1] and the JLAB ERL [2]. Similar to classical coronagraphy, two separate optical channels are arranged with a 2D filter mask at the intermediate image position. In our case the filter mask is a DMD [3], which features a 1024×768 array of micro-mirrors which can be individually addressed to flip  $\pm 12^\circ$  [1]. This unique micro-mirror flipping feature allows us changing the coronagraph mask to adapt to the shape of beam core and achieve the dynamic range required for a given experiment.

Two compensations are applied to easily implement the DMD in the imaging system. The first consists of rotating the DMD  $45^\circ$  about the optical axis of the incident light to orient the micro-mirror 'flip direction' in the horizontal plane. The second is a more subtle effect which requires a horizontal rotation of the CCD camera by the Scheimpflug angle to compensate for the staggered 'array' geometry of the individual DMD micro-mirrors.

At UMER, a dynamic range of  $\sim 10^5$  was measured with this system using a fluorescence source. This system demonstrated the diffraction caused by the DMD mirror array itself had a negligible effect on the image resolution provided the numerical aperture of the second optical channel accepted at least the two primary diffraction orders from the DMD. At the JLAB ERL, we measured the dynamic range of the system to  $\sim 10^7$  using optical

synchrotron radiation (OSR) with the beam halo image to the level of  $10^{-6}$  [2].

The success with the DMD coronagraph at UMER and JLAB encouraged us to apply the DMD masking method to detect the injected beam at SPEAR3 in the presence of the high intensity stored beam. This is important in order to understand the charge capture process and evolution of non-linear beam dynamics in 6-D phase space on a turn by turn basis and allows diagnosis of key beam dynamic effects such as optical beta function matching between the transport line and SPEAR3, charge filamentation and phase-space decoherence.

Nominally, during each 5 min top-up injection cycle, several shots with  $\sim 40-80$  pC/shot are distributed into individual bunches at a 10Hz rate. The ratio between stored charge in a single bunch and the injected pulse is typically 1nC/80pC. Combined with the beam size ratio of  $\sim 100/1$ , the high intensity stored beam will dominate the optical signal on the CCD chip and dramatically reduce the signal to noise ratio of the injected beam which makes it difficult to detect the injected beam. The DMD mask and optical gating are used in combination to resolve the injected beam pulse.

## EXPERIMENTAL SETUP

The visible diagnostic beam line at SPEAR3 [4] contains a rectangular aperture mask about 7 meters from the OSR source point with an angular acceptance of  $3.5 \times 6$  mrad<sup>2</sup>. A  $\pm 0.47$  mrad rectangular 'cold figure' is located right after the primary aperture in order to absorb the intense x-ray core of the beam. This complex compound aperture creates a window-like shape at the first beam line lens and diffraction from the edges of the aperture contributes significantly to the overall shape of the point spread function (PSF) of the optics that is discussed below.

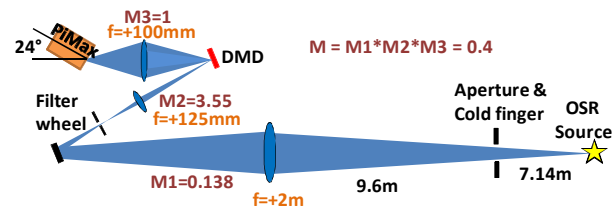


Figure 1: Experimental setup at SPEAR visible OSR beam line.

A schematic of the beam line optics including the 2-channel DMD system is shown in Fig. 1. The image from the source is first imaged to a plane by  $f = 2$  m objective lens and then re-imaged onto the DMD surface by a single acromat,  $f = 125$  mm. At rest the micro-mirrors on the DMD surface are perpendicular to the incident light.

\*Work partially supported by the Office of Naval Research and the DOD Joint Technology Office.

<sup>#</sup>haozhang@umd.edu

The net magnification between the OSR source and the DMD camera is 0.4. This allows us to easily image the  $\pm 8$  mm betatron oscillations of the injected beam onto the 1 cm<sup>2</sup> surface of the DMD. When all the DMD micro-mirrors flip 12° toward the PiMax camera, the incident light will be reflected into the second optical channel which contains a third  $f=100$ mm achromat creating a 1:1 image relay system. Note that the camera is rotated 24° about the vertical axis to compensate for the Scheimplug effect [1].

## EXPERIMENTAL RESULTS

### PSF Measurement

A high dynamic range measurement of the PSF of the optics was performed with the DMD masking technique using the point-like stored beam; the results are shown in Fig. 2. The cross-like structures are due to diffraction from the compound aperture, whose shadow is shown in the insert. Details of the PSF measurement are given in [2].

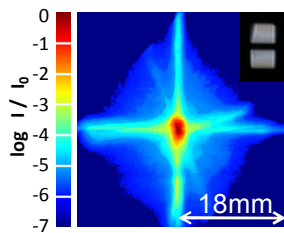


Figure 2: SPEAR3 PSF in log scale; insert: shadow of the compound aperture in the visible SR beam line.

### Injected Beam Imaging

The OSR intensity from the injected beam is not strong enough, even with full MCP gain on the PiMax camera to image on a single pass with only one exposure. Thus, we utilized the synchronously-triggered gate mode of the PiMax to integrate several images per exposure (typically 15) prior to image readout. With stored beam present the problem of rejecting the stored beam light intensity is therefore compounded 15 fold. Two methods are used to reject the intense light in the core of the stored beam: (1) masking the image of the stored beam using the DMD and (2) gating in time on the injected charge. In order to image the injected beam in the presence of the stored beam, an intensity threshold mask or a fixed sized mask is applied on the DMD. To generate the threshold mask we integrated the stored beam intensity over a long-exposure time, i.e. during the injection kicker bump excitation, and then numerically calculated the intensity threshold from the resulting image to define the mask.

For the first set of injected-beam measurements we first filled 15 target buckets with the same amount of stored-beam charge ( $\sim 1$ nC), and then progressively injected a single  $\sim 50$ pC shot into each of them advancing from bucket to bucket each shot. The camera gate was synchronized with the injected beam pulse and automatically advanced from bucket to bucket. We call

this process “clock mode” imaging. This has the advantage that the current of the stored beam in each bunch, which creates the background of each gated image, is kept nearly constant. In the alternative “stacking mode”, in which injected pulses progressively increase the stored charge of a single bunch, there was concern that the increasing current of the stored beam might influence of the injected beam dynamics. Moreover, the “clock mode” is the only way to make online measurements when machine is in dedicated user mode. However, the disadvantage of clock mode is that it is time-consuming, because it is necessary to dump the beam or advance to another group of target bunches (buckets) after the charge in the target buckets becomes excessively high.

Between injected beam shots, the camera trigger interval is 0.1s due to the 10 Hz booster repetition rate, plus an additional  $2.1 \times n$  nano-seconds increment, where 2.1 ns is the time shift between any 2 continuous buckets, and n is the number of buckets between two target buckets. The camera gate was set to 10 ns to only gate the camera on the specific bunch receiving the injected charge. Since the recirculation time in SPEAR3 is 781 ns, we can capture the  $n^{\text{th}}$  turn of the injected beam by setting the camera delay to  $t_0 + 781 \times n$  nano-seconds.

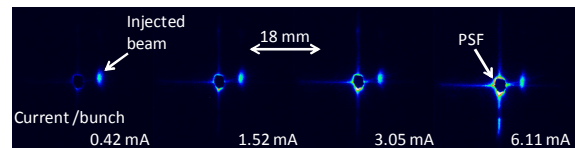


Figure 3: Masked with time-gated images of injected beam turn 6 with increasing single-bunch current.

As illustrated in Fig. 3, we used the “clock mode” technique to image the injected beam at turn 6 for 15 shots and different single-bunch stored beam currents. Here the PSF clearly becomes visible as the stored beam current is increased.

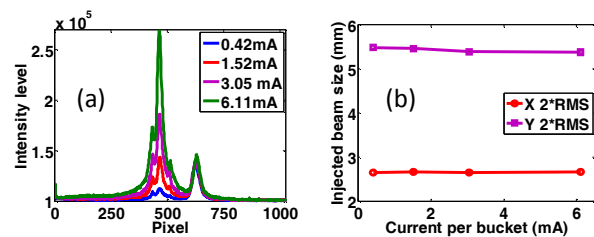


Figure 4: a) Horizontal intensity profile of the injected beam including PSF contribution from stored beam; b)  $2 \times \text{rms}$  injected beam size vs. stored beam current.

Intensity profiles formed by integrating along the vertical axis are shown in Fig. 4 (a). The plots clearly show that with increasing stored beam current the illumination of the PSF (left peak) is enhanced while the intensity profile of the injected beam (right peak) remains nearly constant. The constant profile of the injected beam also demonstrates that at these current levels the injected beam dynamics is not affected by space charge amplitude

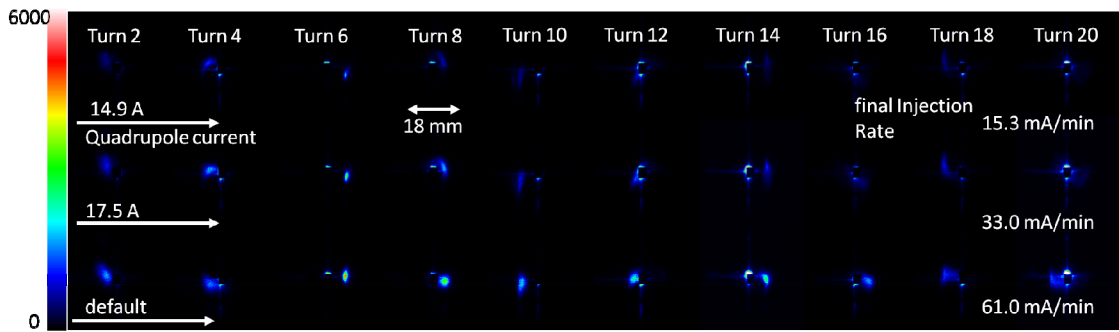


Figure 5: First 20 turns of the injected beam for three cases of matching condition.

in the stored beam. This result is further confirmed by comparing the  $2\times$ rms  $x$ - and  $y$ - beam size profile plotted in Fig. 4 (b), which shows a nearly constant injected beam profile at turn 6, with values about  $x=2.6$  mm and  $y=5.5$  mm.

### Beam Mismatch Experiment

By altering the strength of the 9<sup>th</sup> defocusing quadrupole in the Booster-to-Storage ring (BTS) transport beam line, it is possible to change the phase-space matching of the injected beam with respect to the storage ring and impact charge capture efficiency. For these tests we used the same “clock mode” data acquisition process as before but generated a larger “rectangular” DMD mask instead of an intensity mask because the stored beam had a small residual betatron oscillation after the injection kickers fired.

Fig. 5 shows images of the 20 turns of the injected beam for three different BTS matching conditions. For each condition the plots are delineated by injection rate. The  $x$  and  $y$  centroid motions are plot in Fig. 6 for each case. Clearly the defocusing quadrupole strength has a limited effect on the horizontal betatron motion (dominated by the injection oscillation) but has a large impact in the vertical direction indicating a vertical beam offset in the in defocusing BTS quadrupole.

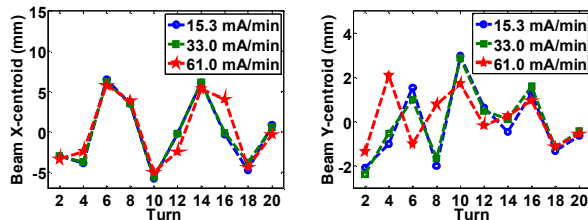


Figure 6: Beam centroid motion of the injected beam for the three different BTS matching condition.

To investigate the phase-space matching, we plot the  $2\times$ rms beam size for each turn in Fig. 7. For both the  $x$  and  $y$  coordinates, the beam sizes are initially similar yet undergo different turn-by-turn evolutions due to different phase-space beam dynamics in each plane. The  $2\times$ rms size is not shown for turns 12, 16 and 20, since the images of the injected beam were partially blocked by the stored beam mask and light from the beam line PSF.

For turns that can be clearly imaged, such as turns 6, 10 and 18, there is a linear relation between the integrated image intensity of the injected beam and the injection rate. This indicates that most of the beam loss occurs in the BTS transport line or in the injection septum prior to entering the storage ring.

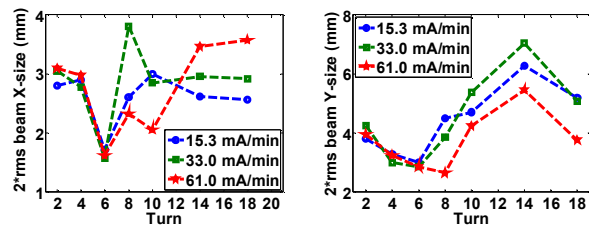


Figure 7: Beam size evolution of the injected beam with three different BTS quadrupole matching conditions.

## CONCLUSION

We have employed a novel DMD masking method to image the visible OSR from the SPEAR3 electron beam with high dynamic range. By blocking out the stored beam to observe the evolution of the injected beam on a turn by turn basis, we are able to study the non-linear injected beam dynamics in the presence of the stored beam. In the future we plan to test the configuration with the full 350ma stored beam during user operations and improve the data acquisition process to allow reconstruction of the injected beam that resides behind the mask or is dominated by the PSF. This work will likely require a modified Lyot stop. Optimal matching of the BTS and a clearer understanding of nonlinear filamentation and decoherence processes will lead to improved capture efficiency at SPEAR3 and storage ring physics in general.

## REFERENCES

- [1] H. Zhang, et.al, ‘Beam Halo Imaging with a Digital Optical Mask’, arXiv:1203.2274v1 [physics.acc-ph].
- [2] R. Fiorito, et.al, ‘Optical Synchrotron Radiation Beam Imaging with a Digital Mask’, Proc. of BIW2012, Newport News, VA, 2012.
- [3] DMD Discovery 4100 Controller Board and Starter Kit, Texas Instruments, Inc.
- [4] W. J. Corbett, et al, ‘Injected Beam Dynamics in SPEAR3’, Proc. of BIW10, Santa Fe NM, 2010.